CellPress

Cell Metabolism
Article

Akt-Dependent Metabolic Reprogramming Regulates Tumor Cell Histone Acetylation

Joyce V. Lee,[1,2,11] Alessandro Carrer,[1,2,11] Supriya Shah,[1,2,11] Nathaniel W. Snyder,[3] Shuanzeng Wei,[4] Sriram Venneti,[5] Andrew J. Worth,[3] Zuo-Fei Yuan,[6] Hee-Woong Lim,[7] Shichong Liu,[6] Ellen Jackson,[1,2] Nicole M. Aiello,[2,8] Naomi B. Haas,[8] Timothy R. Rebbeck,[9] Alexander Judkins,[10] Kyoung-Jae Won,[7] Lewis A. Chodosh,[1,2] Benjamin A. Garcia,[6] Ben Z. Stanger,[2,8] Michael D. Feldman,[4] Ian A. Blair,[3] and Kathryn E. Wellen[1,2,*]

[1]Department of Cancer Biology
[2]Abramson Family Cancer Research Institute
[3]Department of Pharmacology
[4]Department of Pathology and Laboratory Medicine
University of Pennsylvania Perelman School of Medicine, Philadelphia, PA 19104, USA
[5]Memorial Sloan Kettering Cancer Center, New York, NY 10065, USA
[6]Department of Biochemistry and Biophysics
[7]Department of Genetics and Institute for Diabetes, Obesity and Metabolism
[8]Department of Medicine
[9]Department of Biostatistics and Epidemiology
University of Pennsylvania Perelman School of Medicine, Philadelphia, PA 19104, USA
[10]Department of Pathology and Laboratory Medicine, Keck School of Medicine of University of Southern California and Children's Hospital Los Angeles, Los Angeles, CA 90027, USA
[11]Co-first author
*Correspondence: wellenk@exchange.upenn.edu
http://dx.doi.org/10.1016/j.cmet.2014.06.004

SUMMARY

Histone acetylation plays important roles in gene regulation, DNA replication, and the response to DNA damage, and it is frequently deregulated in tumors. We postulated that tumor cell histone acetylation levels are determined in part by changes in acetyl coenzyme A (acetyl-CoA) availability mediated by oncogenic metabolic reprogramming. Here, we demonstrate that acetyl-CoA is dynamically regulated by glucose availability in cancer cells and that the ratio of acetyl-CoA:coenzyme A within the nucleus modulates global histone acetylation levels. In vivo, expression of oncogenic Kras or Akt stimulates histone acetylation changes that precede tumor development. Furthermore, we show that Akt's effects on histone acetylation are mediated through the metabolic enzyme ATP-citrate lyase and that pAkt(Ser473) levels correlate significantly with histone acetylation marks in human gliomas and prostate tumors. The data implicate acetyl-CoA metabolism as a key determinant of histone acetylation levels in cancer cells.

INTRODUCTION

Rewiring of cellular metabolism in cancer cells is crucial for increased macromolecular biosynthesis, growth, and proliferation, and metabolic deregulation is now considered a hallmark feature of cancer cells (Hanahan and Weinberg, 2011; Ward and Thompson, 2012). In addition to directly supporting energetics and biosynthesis, a growing body of evidence suggests that metabolic enzymes may also promote tumorigenesis through functions that are not overtly metabolic. For example, the M2 isoform of pyruvate kinase, a glycolytic enzyme, has been reported to enter the nucleus and serve as transcriptional coregulator (Luo and Semenza, 2012). ATP-citrate lyase (ACLY), a lipogenic enzyme, is also present in the nucleus and plays a crucial role in regulating nuclear acetylation events, including histone acetylation (Wellen et al., 2009).

Metabolic changes in cancer cells are typically mediated by activation of oncogenes and/or loss of tumor suppressors. Hence, mutations that drive tumorigenesis also cause metabolic alterations. In addition to genetic mutations, epigenetic alterations play a key role in enabling malignant transformation and tumor growth (Azad et al., 2013; Shen and Laird, 2013), although mechanisms underlying epigenetic alterations in cancer are not fully clear. Notably, many chromatin-modifying enzymes depend on metabolic intermediates as cofactors or substrates, and certain chromatin modifications have been shown to be sensitive to the cellular metabolic state (reviewed in Kaelin and McKnight, 2013; Katada et al., 2012; Lu and Thompson, 2012; Yun et al., 2012). Links between cancer cell metabolism and DNA and histone methylation have been recently identified in tumors with specific mutations, such as those in isocitrate dehydrogenase (*IDH1* and *IDH2*). Mutant IDH enzymes exhibit altered enzyme activity favoring conversion of α-ketoglutarate (αKG) into (*R*)-2-hydroxyglutarate, a metabolite that inhibits the activity of αKG-dependent JmjC-domain histone demethylases and TET enzymes, resulting in hypermethylation of DNA and histones (reviewed in Losman and Kaelin, 2013; Ward and Thompson, 2012). Succinate dehydrogenase (*SDH*) mutations and nicotinamide N-methyltransferase (NNMT) overexpression also result

in methylation changes in cancer cells (Killian et al., 2013; Letouzé et al., 2013; Ulanovskaya et al., 2013; Xiao et al., 2012). In these specific cases, the epigenetic alterations are a direct result of altered activity of a particular metabolic enzyme. However, it is not known whether metabolism might more universally contribute to tumor epigenetic deregulation.

Histone acetylation is a dynamic chromatin mark, with important roles in gene regulation, DNA damage repair, and DNA replication. Global histone acetylation has also been implicated in contributing to pH balance and postulated to serve as a depot for acetate that could be mobilized as an energy source (Martinez-Pastor et al., 2013; McBrian et al., 2013). The metabolite acetyl coenzyme A (acetyl-CoA) is the required donor substrate used by lysine acetyltransferase (KAT) enzymes. In cells cultured under standard conditions, glucose-derived carbon supplies the majority of acetyl-CoA used for histone acetylation, although glutamine and acetate also contribute (Evertts et al., 2013). In some conditions, fatty acid breakdown can also contribute to nuclear acetyl-CoA and histone acetylation (Donohoe et al., 2012). Acetyl-CoA is compartmentalized into mitochondrial and nuclear-cytoplasmic pools (Takahashi et al., 2006). Production of nuclear-cytoplasmic acetyl-CoA from glucose, glutamine, or fatty acids depends on export of citrate from the mitochondria, where it is cleaved by ACLY to generate acetyl-CoA and oxaloacetate. Acetate also supplies nuclear-cytoplasmic acetyl-CoA through acetyl-CoA synthetase (ACECS1/ACSS2). Together, ACLY and ACECS1 are the primary enzymatic sources of acetyl-CoA outside of the mitochondria. Several studies have demonstrated that histone acetylation levels are highly sensitive to the availability of acetyl-CoA, in cell types from yeast to human (Cai et al., 2011; Donohoe et al., 2012; Friis et al., 2009; Takahashi et al., 2006; Wellen et al., 2009).

Given that production and utilization of metabolites is dramatically altered in cancer cells, and that histone acetylation is responsive to acetyl-CoA availability, we postulated that metabolic reprogramming in tumor cells might alter acetyl-CoA and histone acetylation levels in tumors. In this study, we provide evidence that metabolic reprogramming orchestrated by oncogenic activation of Akt drives changes in acetyl-CoA production and histone acetylation that are reflected in total histone acetylation levels in tumors. This study demonstrates that metabolic reprogramming mediated by oncogenic activation of a signal transduction pathway plays a major role in regulation of the cancer cell epigenome.

RESULTS

Histone Acetylation Is Variably Sensitive to Glucose in Cancer Cells

We previously showed that ACLY plays a key role in determining global histone acetylation levels in cancer cells. Histone acetylation is markedly reduced upon silencing of ACLY and can be restored by supplementing cells with the alternate acetyl-CoA source acetate, indicating that the ability of cells to produce acetyl-CoA can limit histone acetylation (Wellen et al., 2009). To determine whether glucose availability regulates histone acetylation levels in cancer cells, we examined a panel of cancer cell lines, including glioblastoma, prostate cancer, and breast cancer cell lines. Histone acetylation was sensitive to glucose availability in each of the cell lines examined, to varying degrees (Figures 1A and S1A, available online). As we have previously shown in other cell types (Wellen et al., 2009), silencing of ACLY inhibited glucose-dependent histone acetylation in LN229 cells (Figure S1B).

In LN229 glioblastoma cells, proliferation slowed when cultured in 1 mM glucose, but between 2 and 25 mM glucose doubling time was equal, indicating that histone acetylation patterns are regulated by glucose independently of cell proliferation (Figure S1C). Cells remained viable in all conditions (Figure S1C). As glucose was progressively limited, glutamine consumption increased (Figure S1C). Although glutamine can be used to supply nuclear-cytoplasmic acetyl-CoA, LN229 cells failed to sustain high histone acetylation levels in low glucose despite increased consumption of glutamine (Figure 1A).

We next sought to define which histone lysines are most sensitive to glucose availability. LN229 cells were incubated for 24 hr in 1 mM or 10 mM glucose, and histone modifications were analyzed by mass spectrometry. Higher acetylation in 10 mM compared to 1 mM glucose was observed at all H2A, H3, and H4 tail lysines analyzed (Figure S1D and Table S1). To confirm that this is due to reduced glucose carbon incorporation into acetylated histones, this analysis was repeated in 1 mM or 10 mM [U-$^{13}C_6$]glucose. After 24 hr, enrichment was reduced in low glucose for all lysines analyzed (Table S2). However, the effects of glucose limitation became more pronounced as more lysines were acetylated in *cis*. For example, the histone H4 tail can be acetylated at lysines 5, 8, 12, and 16. In 1 mM [U-$^{13}C_6$]glucose, significantly more tetra-acetylated histone H4 (AcH4) tails were enriched at 0 or 1 acetyl group, while in 10 mM, 3 or 4 acetyl groups were more frequently enriched (Figure S1E). Thus, these data indicate that (1) on all tail lysines examined, acetylation is sensitive to glucose availability, and (2) glucose limitation has a greater impact on histone tails with multiple lysines acetylated in *cis*.

Supplementation of acetate restored histone acetylation levels in low glucose conditions (Figure 1B). Correspondingly, acetyl-CoA levels were reduced in low glucose conditions and significantly rescued by addition of acetate (Figure 1C). To determine whether specific gene sets correlated with these effects on histone acetylation, we performed RNA sequencing to identify acetyl-CoA-regulated genes (genes suppressed or induced by low glucose and reversed by acetate). Approximately 10% of glucose-regulated genes were also significantly regulated by acetate (Figure 1D). Clustering analysis revealed that acetate regulated most genes in the same direction as glucose, suggesting that acetyl-CoA is a key mediator of glucose-dependent gene expression (Figure 1E and Table S3). Expression was confirmed for select acetyl-CoA-regulated genes by quantitative PCR (qPCR) (Figure S2A), and chromatin immunoprecipitation (ChIP) analyses at these genes showed that promoter histone acetylation correlated with expression (Figure S2B). Analysis of curated pathways revealed enrichment for genes involved in cell cycle and DNA replication among acetyl-CoA-induced genes, suggesting that acetyl-CoA stimulates a pro-proliferative gene expression profile (Figure 1F). Analogously, prior studies in yeast showed that acetyl-CoA promotes cell growth and division by promoting expression of genes involved in these processes (Cai et al., 2011; Shi and Tu, 2013). Although acetate supplementation was not sufficient to restore normal doubling time in

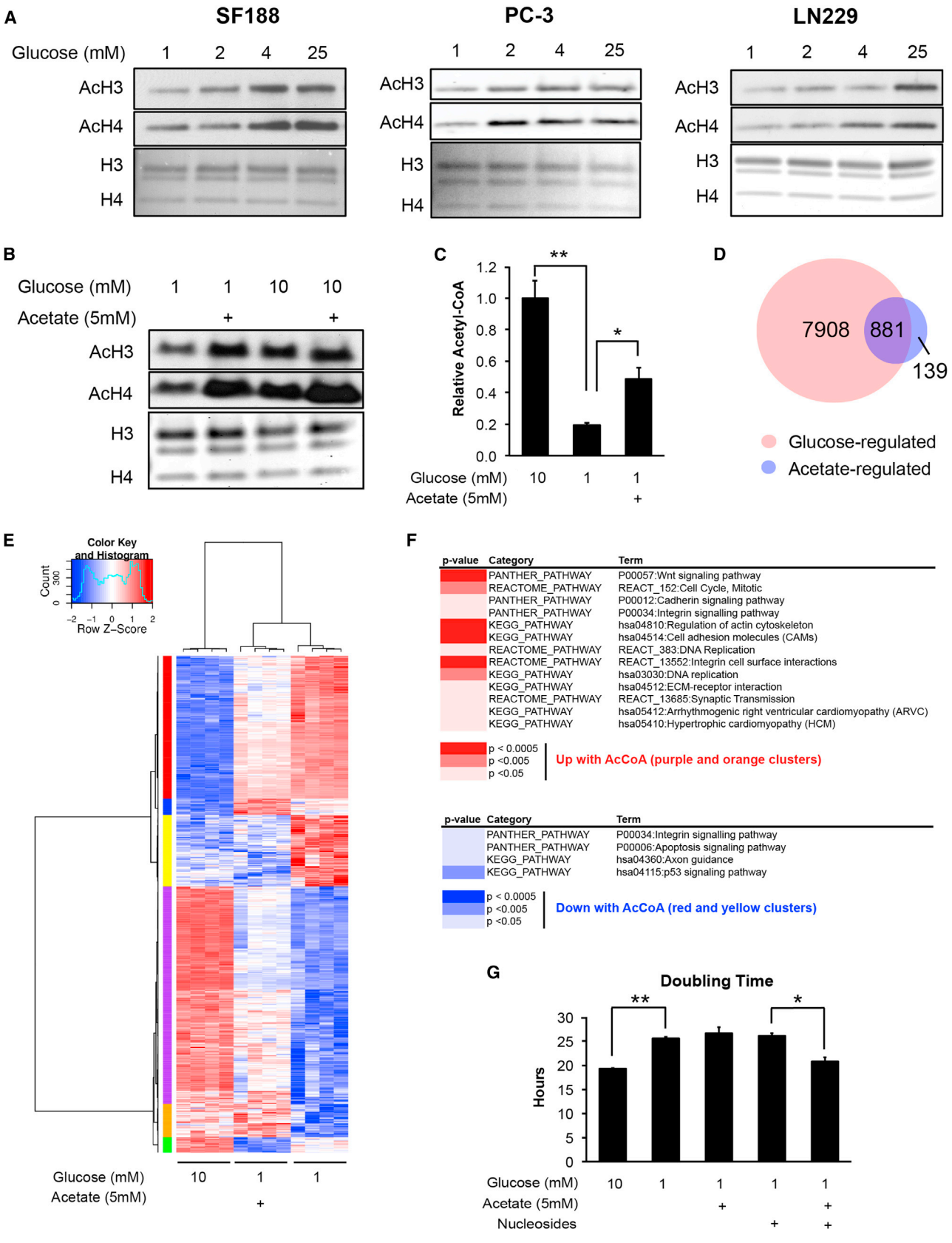

(legend on next page)

low glucose conditions in LN229 cells (Figure 1G), we considered that additional glucose-derived components might be required. Indeed, supplementation of acetate together with nucleosides (synthesis of which requires ribose generated in the pentose phosphate pathway) rescued doubling time, while neither component alone did so (Figure 1G). These data suggest that acetyl-CoA facilitates expression of proliferation-related genes as part of an integrated growth response.

Acetyl-CoA and Coenzyme A Are Key Determinants of Histone Acetylation in Cancer Cells

If acetyl-CoA serves as a signal of nutrient sufficiency to promote growth and proliferation, cells must have mechanisms to detect changes in acetyl-CoA abundance. Work in yeast has shown that Gcn5 is crucial for mediating histone acetylation in response to acetyl-CoA availability (Cai et al., 2011; Friis et al., 2009). In yeast, acetyl-CoA concentrations oscillate within a range that could plausibly regulate yeast Gcn5, which has a K_D of 8.5 μM (Cai et al., 2011). However, human GCN5 binds acetyl-CoA much more tightly (K_D of 0.56 μM) (Langer et al., 2002). This suggests either that levels of acetyl-CoA are lower in human cells than in yeast or that the absolute concentration of acetyl-CoA is not the key regulatory factor for overall histone acetylation levels in human cells. Notably, many lysine acetyltransferases (KATs) including GCN5 are inhibited by the product CoA and bind acetyl-CoA and CoA with similar affinities. Hence, it has been postulated that the ratios of these metabolites might be the critical determinant for overall histone acetylation levels (Albaugh et al., 2011).

We therefore measured absolute acetyl-CoA and CoASH (reduced CoA) concentrations, normalized to cell volume, in LN229 cells cultured in 1 or 10 mM glucose. Acetyl-CoA was measured at 6–13 μM in high glucose conditions and fell to 2–3 μM in low glucose. CoASH tended to rise in low glucose, and the ratio of acetyl-CoA:CoASH was found to be ~1.5–2 throughout the time course in high glucose conditions and to fall below 1 under low glucose (Figure 2A). We also examined acetyl-CoA and CoASH levels in a second cell line, IL-3-dependent hematopoietic cells, since the volume of these cells under standard conditions and during nutrient and growth factor withdrawal has been extensively characterized (Lum et al., 2005; Wellen et al., 2010). A similar range of acetyl-CoA concentrations (~3–12 μM) were measured in these cells as in LN229 cells, and both acetyl-CoA and acetyl-CoA:CoASH were significantly reduced when cells were deprived of either glucose or growth factor (Figure 2B). The range of acetyl-CoA concentrations observed in each of these cell lines is comparable to that reported over the yeast metabolic cycle (Cai et al., 2011).

To specifically test whether histone acetylation levels respond to both acetyl-CoA and CoA levels, nuclei were isolated from LN229 cells and incubated with defined concentrations of acetyl-CoA and CoASH, which can freely enter the nucleus through the nuclear pore complex. We observed that in the presence of high acetyl-CoA, addition of CoASH suppressed histone acetylation in a dose-dependent manner (Figure 2C). Together, these data indicate that levels of both acetyl-CoA and CoA in the nucleus can impact histone acetylation levels. Moreover, the ratio of acetyl-CoA:CoASH is glucose sensitive and tracks with total acetyl-CoA.

Expression of $Kras^{G12D}$ in the Mouse Pancreas Promotes Increased Histone Acetylation Prior to Tumor Development

Since histone acetylation is sensitive to metabolic state and metabolism is altered in cancer cells, we next asked whether oncogene activation could drive changes in histone acetylation in vivo. Oncogenic *KRAS* mutations are found in the vast majority of human pancreatic adenocarcinoma (PDA) cases, and recent studies have demonstrated that mutant Kras in pancreatic cancer cells drives extensive metabolic rewiring (Son et al., 2013; Ying et al., 2012). We observed that in the pancreas of healthy wild-type (WT) mice, acinar cells exhibited very low levels of AcH3 and AcH4, as detected by immunohistochemistry (IHC), although ductal cells were strongly positive for these marks (Figure 3A). In contrast, in mice expressing oncogenic Kras ($LSL\text{-}Kras^{G12D}$; $p53^{L/+}$; Pdx1-Cre [KPC] mice), areas of acinar-to-ductal metaplasia (ADM), precancerous pancreatic intraepithelial neoplasia (PanIN), and PDA exhibited high levels of AcH3 and AcH4 (Figure 3A and 3B). PDA may arise from acinar cells (Morris et al., 2010), and strikingly, elevated AcH4 was observed in acinar cells even prior to increases in proliferation, as assessed by Ki67 immunostaining (Figure 3C) or the appearance of any histological abnormalities (Figures 3A and S3). Thus, histone acetylation levels are elevated upon $Kras^{G12D}$ expression in mouse pancreas early in the process of tumor development.

We next interrogated signaling pathways downstream of Kras to identify those responsible for elevating histone acetylation in primary murine PanIN cells. Reductions in histone acetylation were observed with each of the inhibitors that we tested (Figure 4A). Phosphatidylinositol 3-kinase (PI3K) and Akt inhibition also significantly reduced glucose uptake and lactate consumption and suppressed Acly phosphorylation (Figures 4A and 4B). Phosphorylation at Ser455 has been shown to increase ACLY's activity (Potapova et al., 2000). On the other hand, the level of AceCS1, which produces nuclear-cytoplasmic acetyl-CoA from acetate, was somewhat suppressed by PI3K, but not by Akt, inhibition in these cells (Figure 4A). Acetyl-CoA and acetyl-CoA:CoASH levels were potently suppressed upon Akt inhibition (Figure 4C), and histone acetylation levels in Akt inhibitor-treated

Figure 1. Glucose Availability Regulates Histone Acetylation in Several Cancer Cell Lines

(A) Acetylation of acid-extracted histones from cells cultured under indicated glucose conditions for 24 hr. Total histones were stained by Coomassie or Ponceau.
(B) Acetylation of acid-extracted histones from LN229 cells treated with 1 or 10 mM glucose, with or without 5 mM NaOAc for 24 hr.
(C) Relative levels of acetyl-CoA in LN229 cells after 24 hr of indicated treatment; mean ± SEM of triplicates (*$p < 0.05$; **$p < 0.005$).
(D) Venn diagram of genes regulated by glucose and/or acetate in LN229 cells, with the overlap representing genes designated as acetyl-CoA regulated.
(E) Heatmap of 881 genes represented in the overlap from the Venn diagram. See Table S3 for associated gene list and cluster ID.
(F) DAVID functional annotation of pathways regulated by acetyl-CoA, using the gene list identified from the indicated clusters on the heatmap.
(G) Doubling time for LN229 cells treated as indicated for 24 hr; mean ± SEM of triplicates (*$p < 0.05$; **$p < 0.005$).

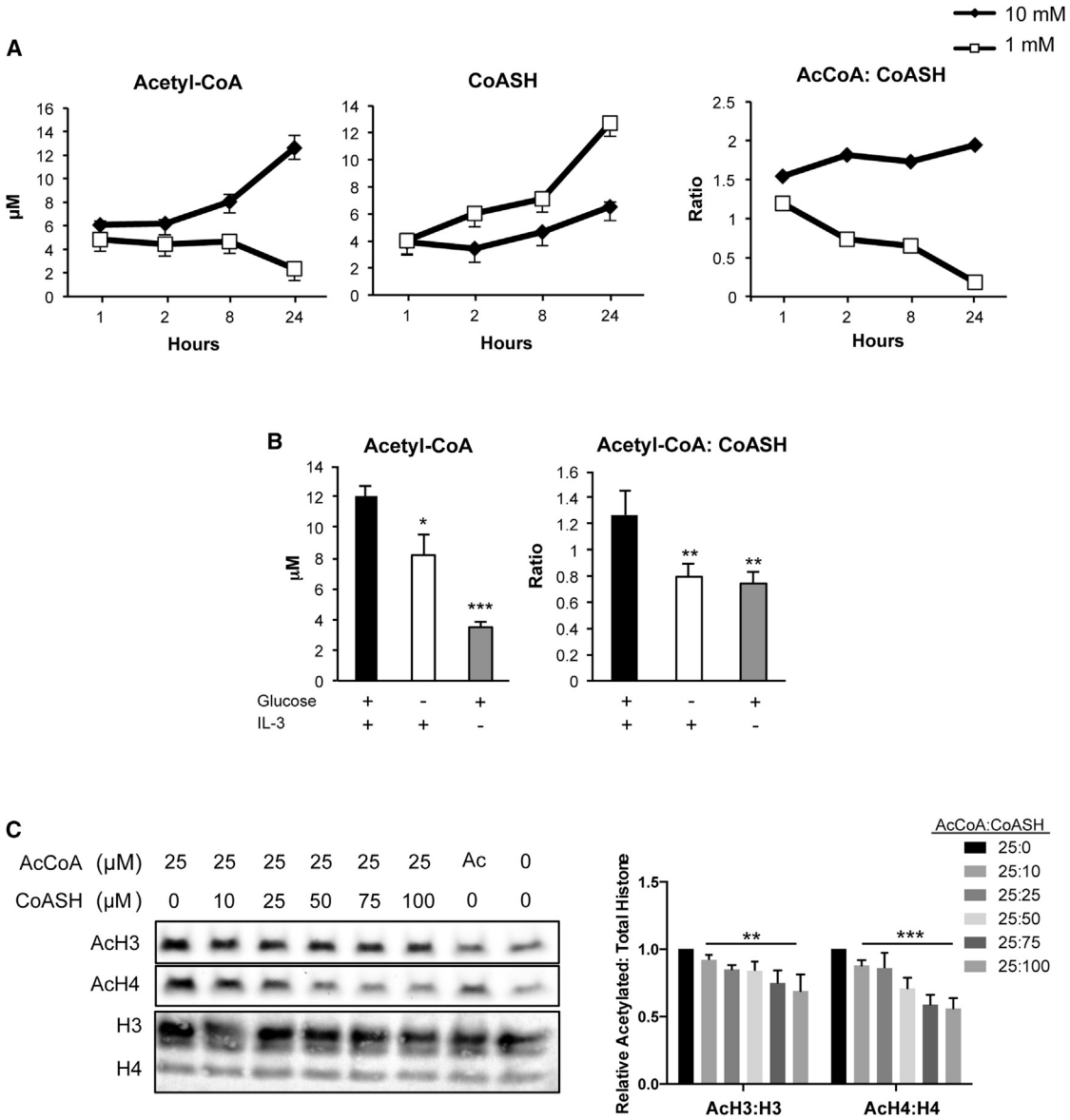

Figure 2. Acetyl-CoA:CoASH Ratio Is a Determinant of Histone Acetylation in Cancer Cells

(A) Molar concentrations of acetyl-CoA, CoASH, and ratio of acetyl-CoA:CoASH over 24 hr in LN229 cells; mean ± SEM of triplicates. Result is representative of three independent experiments.

(B) Interleukin-3 (IL-3)-dependent *Bax*$^{-/-}$*Bak*$^{-/-}$ cells were cultured for 48 hr with or without glucose and with or without IL-3 as indicated. Acetyl-CoA and CoASH were measured and normalized to cell volume; mean ± SD of triplicates. Significance as compared to Glc^{+}IL-3^{+} samples (*$p < 0.05$, **$p < 0.005$, ***$p < 0.0005$).

(C) Representative western blot of acetylated histones upon incubation of isolated nuclei with varying concentrations of acetyl-CoA and CoASH. Total histones were stained by Ponceau. Data were quantified from four independent experiments with 25:0 value set to 1; mean ± SEM. Repeated-measures one-way ANOVA with posttest for linear trend was performed for 25:10–25:100 values. Posttest for linear trend significance for AcH4:H4, ***$p < 0.0001$; for AcH3:H3, **$p = 0.0034$.

cells increased upon supplementing cells with acetate (Figure 4D). Suppression of histone acetylation by Akt inhibition was comparable to that observed upon either glucose limitation or Acly silencing, both of which were also rescued by acetate (Figure 4D). In primary murine PDA cells, we similarly observed suppression of histone acetylation and glucose uptake by PI3K or Akt inhibition, as well as acetate rescue of histone acetylation in Akt inhibitor- or low glucose-treated cells (Figure S4B–S4D). These data indicate that in premalignant and cancerous cells expressing oncogenic Kras, histone acetylation is regulated in part by Akt-dependent regulation of acetyl-CoA metabolism.

Akt Activation Sustains Histone Acetylation in Nutrient-Limited Conditions

To probe further into the mechanism by which Akt regulates histone acetylation, we examined the effects of constitutive Akt activation in cancer cells by comparing parental LN229 cells with LN229 cells in which a constitutively active form of Akt,

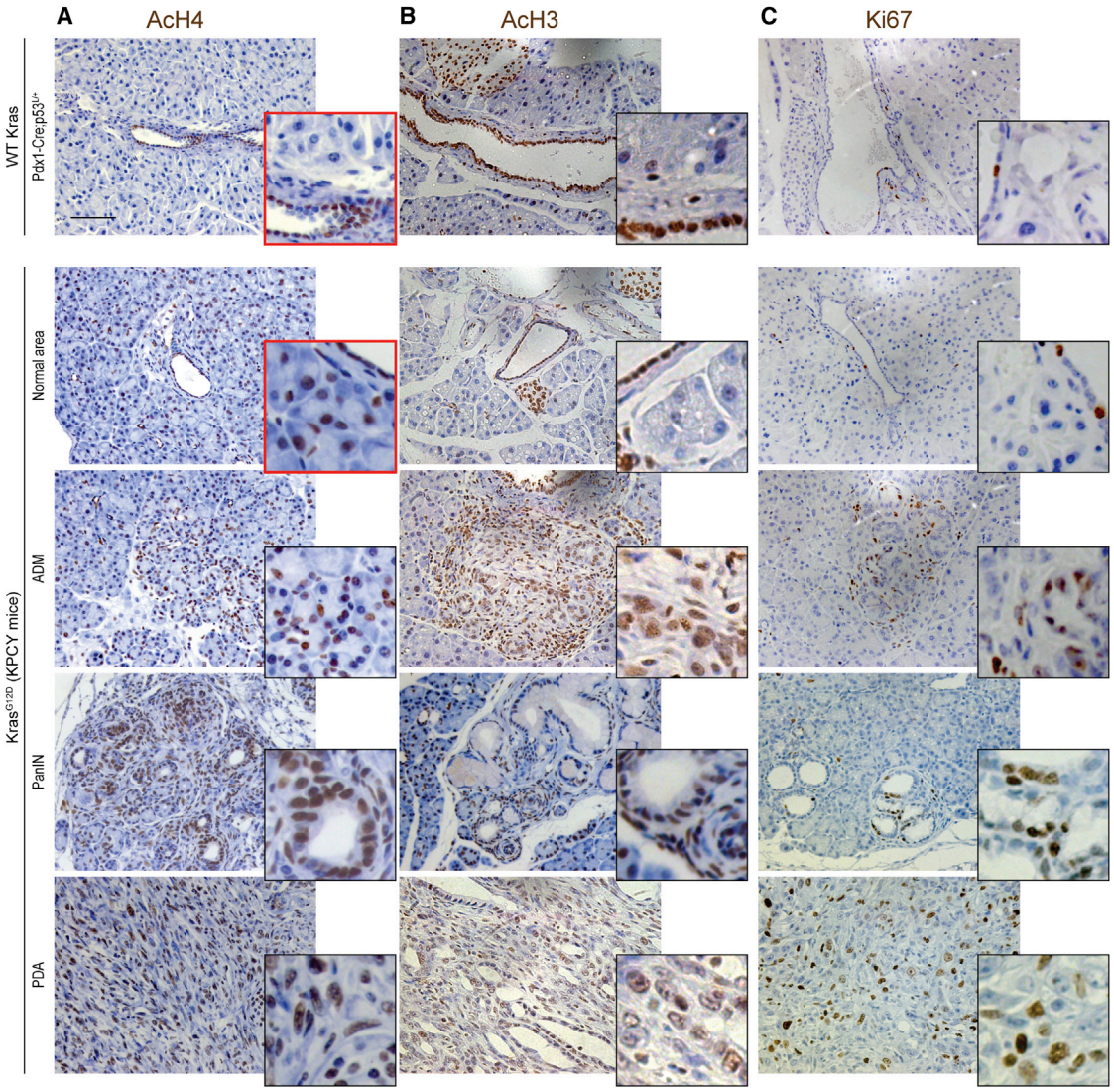

Figure 3. Oncogenic Kras Increases Histone Acetylation In Vivo

(A–C) Pancreata from mice expressing Kras-G12D (KPCY, previously described; Rhim et al., 2012) were harvested at either 6 weeks (KPCY-Normal Area), 8 weeks (KPCY-PanIN), or ≥10 weeks (KPCY-PDA) of age, along with pancreata from control (Kras WT) mice ($n \geq 3$ for each group). Immunohistochemistry against AcH4 (A), AcH3 (B), or Ki67 (C) was performed on paraffin-embedded tissue sections, and nuclei were counterstained with hematoxylin. Representative images are shown, with magnification of areas of interest. Scale bar, 50 μm. See Figure S3 for quantification of AcH4 in acinar cells in Kras WT and KPCY mice.

myristoylated Akt (myrAkt), was stably expressed. LN229-myrAkt cells have been shown to consume more glucose but maintain a proliferation rate similar to that of parental cells (Elstrom et al., 2004). Levels of histone acetylation in high glucose conditions were not markedly different between the two cell lines. However, when cultured in low glucose, LN229-myrAkt cells sustained a level of histone acetylation significantly higher than that of parental cells (Figure 5A). Similar results were also obtained in SF188 and SF188-myrAkt cells (Figure S5A). Time course analysis indicated that myrAkt expression extended the time frame over which cells could maintain histone acetylation levels in low glucose (Figure S5B).

Glucose deprivation results in depletion of ACLY's substrate citrate in LN229 cells (Figure S6A). In myrAkt-expressing cells, citrate levels were lower than in the parental cells, even in high glucose conditions, and loss of citrate was accelerated upon glucose deprivation (Figure S6A). In vitro studies of ACLY enzymatic activity have demonstrated that phosphorylation at Ser455 increases the enzymatic activity of ACLY, resulting in a 6-fold increase in V(max) (Potapova et al., 2000). Hence, increased phosphorylation of ACLY by Akt could potentially enable sustained acetyl-CoA production and thereby histone acetylation even if availability of the ACLY substrate citrate is reduced. To test whether ACLY phosphorylation is sufficient to sustain high levels of histone acetylation in low glucose, we expressed WT Acly and Acly Ser455 phosphomimetic (S455D) and phosphomutant (S455A) proteins in LN229 cells. Expression of Acly-S455D enabled high levels of histone acetylation to be sustained in

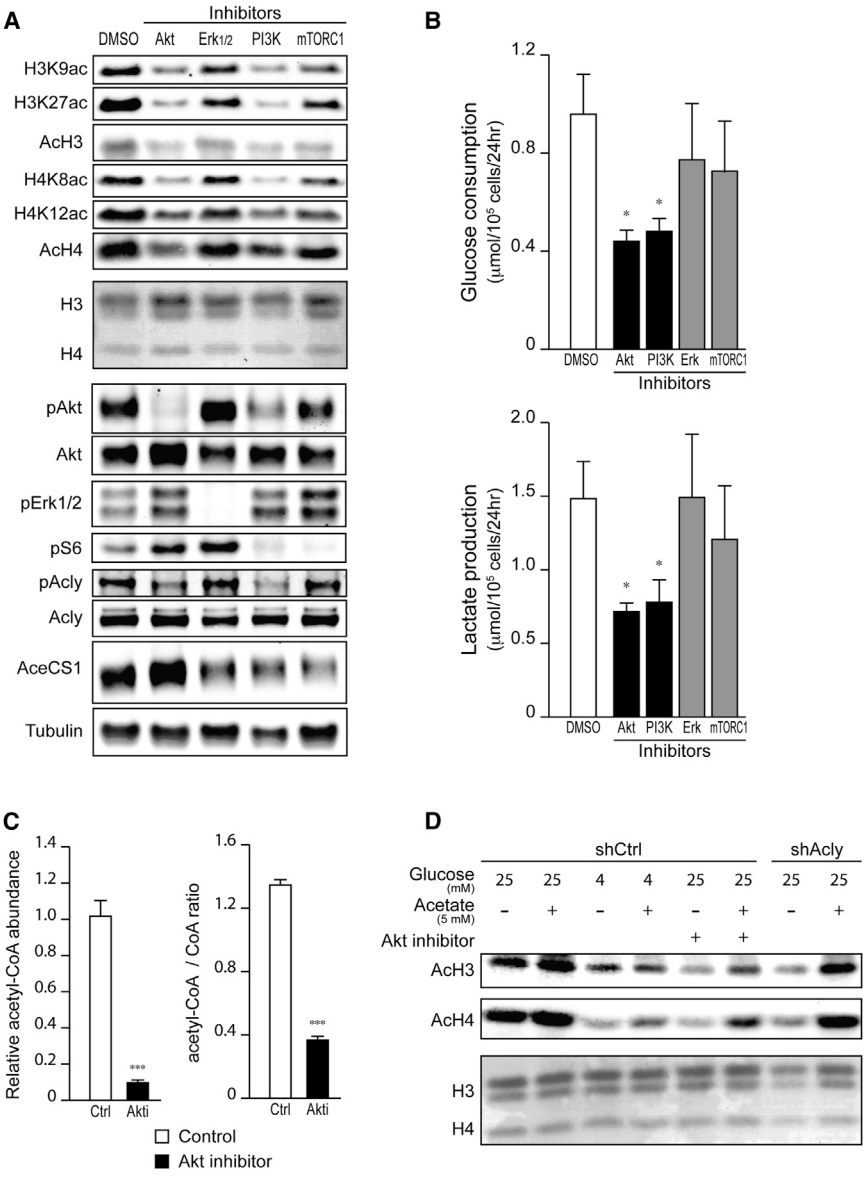

Figure 4. Oncogenic Kras Enhances Histone Acetylation In Vitro in an Akt- and Acly-Dependent Manner

(A) Mouse pancreatic primary cells derived from KPCY mouse PanIN lesions were treated with the indicated inhibitors for 24 hr. Acetylation of histones and phosphorylation of signaling proteins were assessed by western blot in acid extracts and RIPA lysates, respectively. Ponceau staining is shown as loading control for histones.

(B) Glucose consumption and lactate production were measured in PanIN-derived primary mouse cells treated as in (A); mean ± SD of triplicates (*$p < 0.05$).

(C) Acetyl-CoA and CoASH levels were measured in PanIN cells, with or without Akt inhibitor; mean ± SD of triplicates (***$p < 0.001$).

(D) PanIN-derived primary cells were transduced with control (shCtrl) or Acly-targeting (shAcly) short hairpin RNA. Cells were cultivated under indicated glucose concentrations, with or without Akt inhibitor and with or without 5 mM acetate for 24 hr. Histones were acid extracted and analyzed by western blot. Ponceau staining is shown as loading control for histones.

low glucose, similar to that observed with myrAkt expression (Figure 5B). A trend toward higher histone acetylation in low glucose was also noted with expression of WT Acly. These results suggest that ACLY is a key downstream effector of Akt in promoting histone acetylation, particularly when nutrients are limited.

This result raised the question of where cells obtain the carbon for histone acetylation in cells with constitutive Akt/ACLY activation but limited glucose. Recent studies have shown that under certain conditions such as hypoxia, glutamine can be reductively carboxylated to generate citrate and supply lipogenic acetyl-CoA and that depletion of citrate or an elevated α-ketoglutarate:citrate ratio is necessary for this effect (Fendt et al., 2013; Gameiro et al., 2013). We hypothesized that citrate depletion observed with myrAkt expression might stimulate glutamine reductive carboxylation. However, analysis of citrate isotopologues following exposure to [$^{13}C_5$ $^{15}N_2$]glutamine revealed that glutamine continues to be oxidized in myrAkt-expressing cells and that little to no reductive carboxylation occurred in either high or low glucose conditions (Figure S6B). On the other hand, acetyl-CoA, though significantly depleted in control or WT Acly-expressing cells in low glucose, retained a comparable percent of enrichment from glucose (m+2 acetyl-CoA) when cultured in either 1 mM or 10 mM [U-$^{13}C_6$]glucose (Figure 5C). Moreover, in Acly-S455D-expressing cells, both total and m+2 acetyl-CoA resisted depletion in low glucose (Figure 5C), suggesting that even when glucose is limited, it remains a major source of acetyl-CoA in this context.

Hence, the data indicate that Akt promotes acetyl-CoA production and histone acetylation through combined effects on (1) promoting the uptake and metabolism of glucose and (2) promoting phosphorylation and activation of ACLY to facilitate continued acetyl-CoA production even when its substrate citrate is limited.

Akt Activation Acutely Promotes Histone Acetylation In Vivo

To directly test whether acute activation of Akt regulates histone acetylation in vivo, we exploited a doxycycline-inducible mouse model of breast cancer in which myrAkt is activated in mammary epithelial cells upon administration of doxycycline to mice through the drinking water (Gunther et al., 2002). pAkt and pAcly levels increased with myrAkt expression, as expected (Figure 5D). In control animals, relatively weak staining for AcH4 was detected in ductal epithelial cells. Remarkably, however,

upon induction of Akt, pronounced increases in histone acetylation were detected within 96 hr of doxycycline administration (Figure 5D). On the other hand, another activating mark, H3K4me1, was not obviously regulated, suggesting that histone acetylation—not histone marks in general—may be specifically impacted by Akt activation. Hence, acute activation of Akt in vivo increases global histone acetylation levels.

These data indicate that activation of Akt acutely promotes histone acetylation. We next investigated whether Akt activation is associated with histone acetylation in established human tumors.

Histone Acetylation Levels Correlate with pAKT in Human Glioma

The PI3K/Akt pathway is frequently activated in glioblastoma multiform (GBM), due to epidermal growth factor receptor (*EGFR*) or phosphatase and tensin homolog (*PTEN*) mutations (Lino and Merlo, 2011). We examined a diverse panel of human gliomas to determine whether AcH4 is associated with pAKT levels. A total of 56 samples on a tumor tissue microarray (TMA) were analyzed for pAKT and AcH4 (Figure 6A). Each tumor sample was scored in a blinded manner by a neuropathologist and given a combined score for the percentage of positive cells and intensity of staining (H score) for both pAKT and AcH4. A statistically significant positive correlation was found between pAKT and AcH4, indicating that AKT activation is associated with increased histone acetylation in human tumors (Figure 6B). pAKT levels tended to increase with tumor grade, particularly in astrocytomas, although no significant relationship was observed between tumor grade and AcH4 (Figure 6C). The relationship between pAKT and AcH4 is therefore not secondary to effects of tumor grade. *IDH1* (and to a lesser extent *IDH2*) mutations occur frequently in gliomas and alter both cell metabolism and epigenetics (Losman and Kaelin, 2013). Of particular relevance, *IDH* mutations cause hypermethylation of histones (Lu et al., 2012), suggesting the possibility that histone acetylation might be altered secondarily to methylation effects in *IDH* mutant tumors. H3K9me3 was previously shown to be elevated in *IDH* mutant tumors in this patient set (Venneti et al., 2013a), and we found no significant relationship between H3K9me3 and pAKT levels (data not shown). Moreover, AcH4 levels were not different between *IDH* WT and *IDH* mutant tumors (Figure 6D).

Histone Acetylation Levels Correlate with pAKT in Human Prostate Cancer

In human prostate tumors, significant correlations have been reported between levels of histone acetylation marks with tumor grade (H3K18ac and H4K12ac) as well as with the risk of tumor recurrence (H3K18ac, H3K9ac, and H4K12ac) (Bianco-Miotto et al., 2010; Seligson et al., 2005). The PI3K/Akt pathway is frequently activated in prostate cancer due to *PTEN* loss or other mutations, and inhibition of Akt in the PTEN null prostate cancer cell lines PC-3 and C4-2 reduced overall levels of histone acetylation (Figure S7A). We investigated levels of three histone acetylation marks (H3K18ac, H3K9ac, and H4K12ac) and their association with pAKT(Ser473) in a panel of human prostate tumors (Figure 7A). The cohort consisted of patients with either metastatic or localized disease, with primary tumor grades ranging from 3 to 5 on the Gleason scale. Tumors were scored for both the percentage of positive cells and the intensity of staining. A striking positive correlation was observed between pAKT and each of the histone acetylation marks (Figure 7B). Levels of each histone acetylation mark were also strongly correlated with one another in tumors (Figure S7B). Percentages of nuclei positive for H3K18ac were similar between patients with metastatic as compared to localized disease, while H3K9ac and particularly H4K12ac scored positive in a higher percentage of nuclei in patients with metastatic disease (Figure S7C). H4K12ac was also higher in Gleason 4 and 5 tumors than in Gleason 3 samples (Figure S7D). Together, the data from human prostate cancer and glioma suggest that AKT activation is a major determinant of histone acetylation levels in tumors.

Histone Acetylation as a Predictive Biomarker for Therapeutic Failure

For ten of the prostate cancer patients with localized disease, biochemical failure (PSA recurrence) data were available. Strikingly, levels of histone acetylation were highly predictive of which patients would later exhibit biochemical failure. The five patients with the lowest levels of H4K12ac, H3K18ac, and H3K9ac developed biochemical failure, whereas the five with the highest levels of these marks did not (Figure 7C). These findings agree with those of Seligson et al. (2005), showing that low levels of histone modifications such as H3K18ac are associated with a poor prognosis in prostate cancer. Within these ten samples, the relationship between pAKT and each histone acetylation mark held (Figure S7E), although pAKT levels did not predict biochemical failure in these ten samples (Figure 7C). Hence, histone acetylation levels might be a valuable biomarker to predict tumor relapse.

DISCUSSION

We report that oncogenic Akt activation is a key determinant of global histone acetylation levels in cancer cells. We provide evidence that this occurs through Akt-dependent metabolic reprogramming to promote high acetyl-CoA production. Akt ensures continuous acetyl-CoA production even during nutrient limitation by promoting the phosphorylation and activation of ACLY. This report implicates metabolic reprogramming mediated by oncogenic activation of a signal transduction pathway as a major factor underlying tumor epigenomic regulation.

Elucidating the regulation of tumor histone acetylation levels is important clinically, and the mechanisms that control tumor histone acetylation are currently poorly understood. Our data suggest that metabolic effects contribute to determining histone acetylation levels in tumors. Other relevant factors in addition to acetyl-CoA metabolism include levels of KATs and histone deacetylases (HDACs), as well as tumor pH. The significance of global histone acetylation levels is not yet fully clear. Several studies have examined the relationship between histone acetylation levels and tumor recurrence and patient survival in various cancer types (reviewed in Chervona and Costa, 2012; Kurdistani, 2007). Significant correlations have been shown in several studies, although high histone acetylation has been associated with both better and worse prognoses, likely reflecting differences in types of cancer, tumor grade, therapeutic approaches, and sample stratification. Our data suggest that low levels of histone acetylation may predict poor patient outcome in prostate

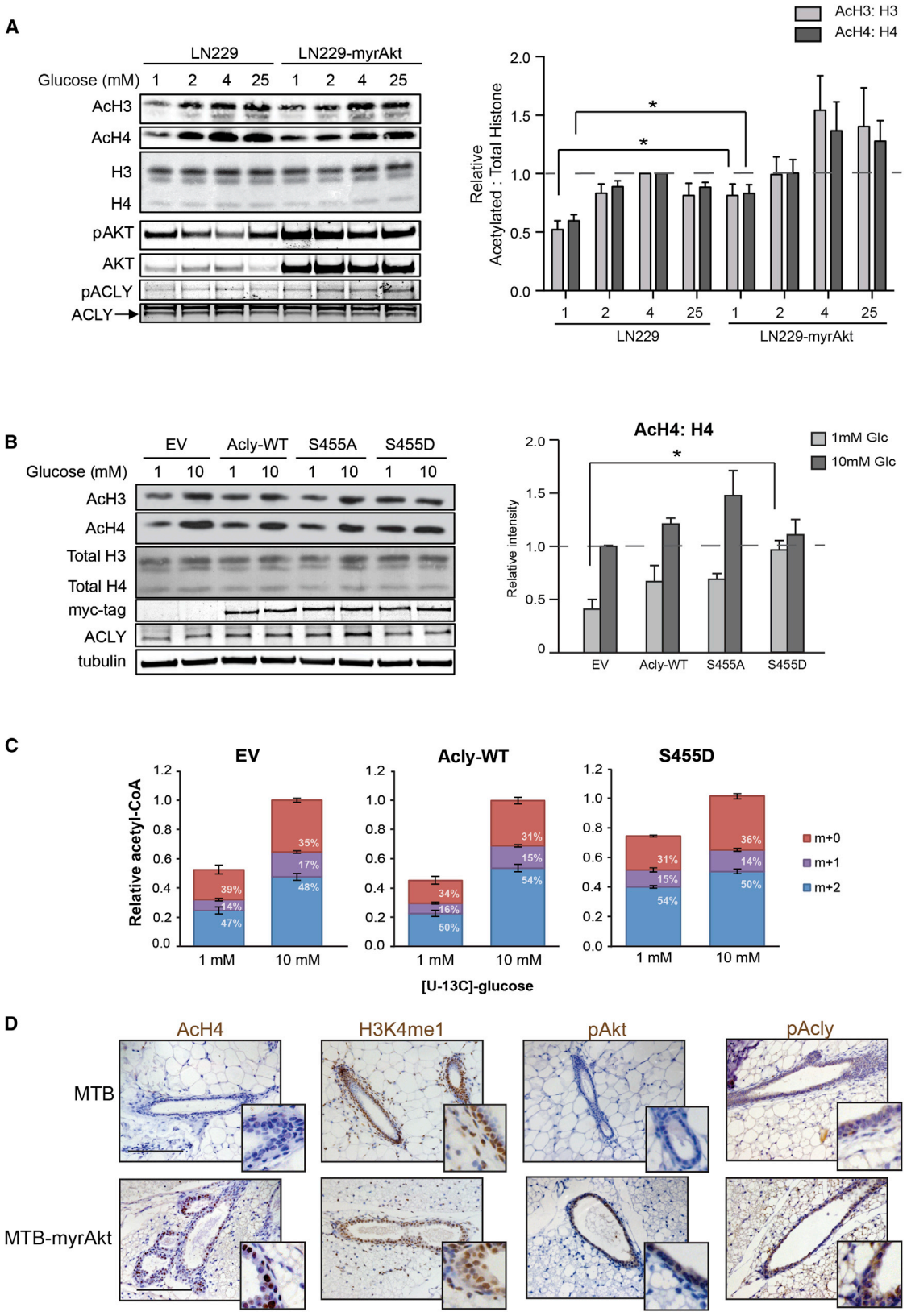

(legend on next page)

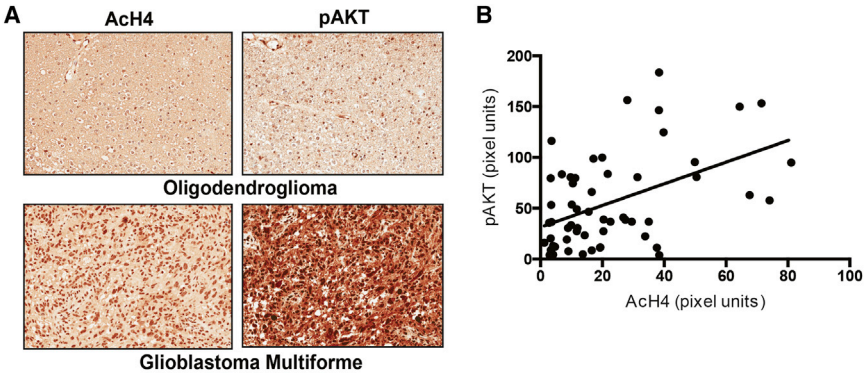

Figure 6. pAKT Correlates with Histone Acetylation in Human Glioma

(A) Representative images (20×) of pAKT and AcH4 in a grade IV GBM and a grade II oligodendroglioma.

(B) pAKT expression showed a significant correlation with AcH4 levels in 56 human glioma samples ($r = 0.4721$, $p = 0.0002$).

(C) pAKT and AcH4 in astrocytic tumors (grade IV astrocytomas = GBM) and oligodendrogliomas; mean ± SD.

(D) pAKT and AcH4 levels in 10 *IDH* mutant and 21 *IDH* WT gliomas; mean ± SD.

cancer, similar to the findings of Seligson et al. (2005). Further study is needed to understand how global histone acetylation levels impact tumor growth and progression as well as treatment responses.

It will be crucial to further investigate the functions of metabolic control of acetylation, as well as the role of ACLY levels and phosphorylation, in regulating gene expression and promoting tumorigenesis. ACLY silencing is known to inhibit cancer cell proliferation and suppress tumor growth (Bauer et al., 2005; Hatzivassiliou et al., 2005; Migita et al., 2008). While suppression of de novo lipogenesis in the absence of ACLY is certainly a key component of this antitumor effect, a growing body of literature indicates that acetylation also plays a crucial role in promoting anabolic metabolism and growth. Acetyl-CoA has been shown to promote growth and proliferation in yeast, through histone acetylation at genes involved in these processes (Cai et al., 2011; Shi and Tu, 2013). Moreover, acetyl-CoA and acetylation regulate many metabolic enzymes (Guan and Xiong, 2011), and a role for acetyl-CoA in suppressing autophagy has also recently been uncovered (Eisenberg et al., 2014; Mariño et al., 2014). We show here that many proliferation-related genes are acetyl-CoA regulated in glioblastoma cells, correlating with overall histone acetylation levels as well as histone acetylation at these genes. Thus, our study adds to a growing body of literature that implicates acetyl-CoA in providing pro-growth cues to the cell.

We have focused this study on the role of the PI3K/Akt pathway in regulation of acetyl-CoA production and histone acetylation. Many oncogenes and tumor suppressors are now recognized to regulate cellular metabolism. Microenvironmental conditions such as hypoxia also potently reprogram cellular metabolism. Moreover, in addition to acetyl-CoA, metabolites such as UDP-GlcNAc, S-adenosylmethionine (SAM), and α-ketoglutarate are also required by chromatin-modifying enzymes and could potentially impact the epigenome if their levels are altered in tumors (Lu and Thompson, 2012). It is therefore conceivable that altered metabolite utilization substantially alters chromatin in many or most cancer cells.

Intense effort is currently aimed at targeting both cancer cell metabolism and cancer epigenetics (Dawson and Kouzarides, 2012; Vander Heiden, 2011). If metabolism is indeed a critical mediator of cancer cell epigenetic deregulation, it is possible that epigenetic alterations could be reversed through therapeutics directed at metabolic targets. Improved understanding of metabolic regulation of the epigenome could point toward contexts in which existing epigenetic therapies, such as HDAC inhibitors, would be most effective or could open doors to development of more specific therapeutics targeting the intersection

Figure 5. Akt Activation Allows Sustained Histone Acetylation in Glucose-Limited Conditions

(A) Western blot analysis of proteins and histones from LN229 and LN229-myrAkt cells. Quantitation represents five independent experiments with LN229 4 mM samples set to 1; mean ± SEM (*$p \leq 0.05$).

(B) Western blot analysis of histone acid extracts from LN229 cells stably expressing vector (EV), WT Acly, Acly-S455A, or Acly-S455D. Cells were treated with 1 or 10 mM glucose for 24 hr before lysis. Quantitation represents the ratio of acetylated to total histones in four independent experiments with EV 10 mM set to 1; mean ± SEM (*$p < 0.05$).

(C) Relative acetyl-CoA concentrations and percent enrichment after treatment in 1 mM or 10 mM [U-$^{13}C_6$]glucose for 20 hr; mean ± SEM of triplicates. Total acetyl-CoA levels as well as m+2 acetyl-CoA (enriched from glucose) were significantly suppressed ($p < 0.05$) in 1 mM as compared to 10 mM glucose in EV and WT-Acly cells, but not Acly-S455D cells.

(D) Control (MTB) and transgenic (MTB-tAkt) mice were administered doxycyclin for 96 hr ($n \geq 5$ for each group). Immunohistochemistry was performed on paraffin-embedded mammary tissue sections. Representative images are shown, along with magnification of areas of interest. Scale bar, 50 μm.

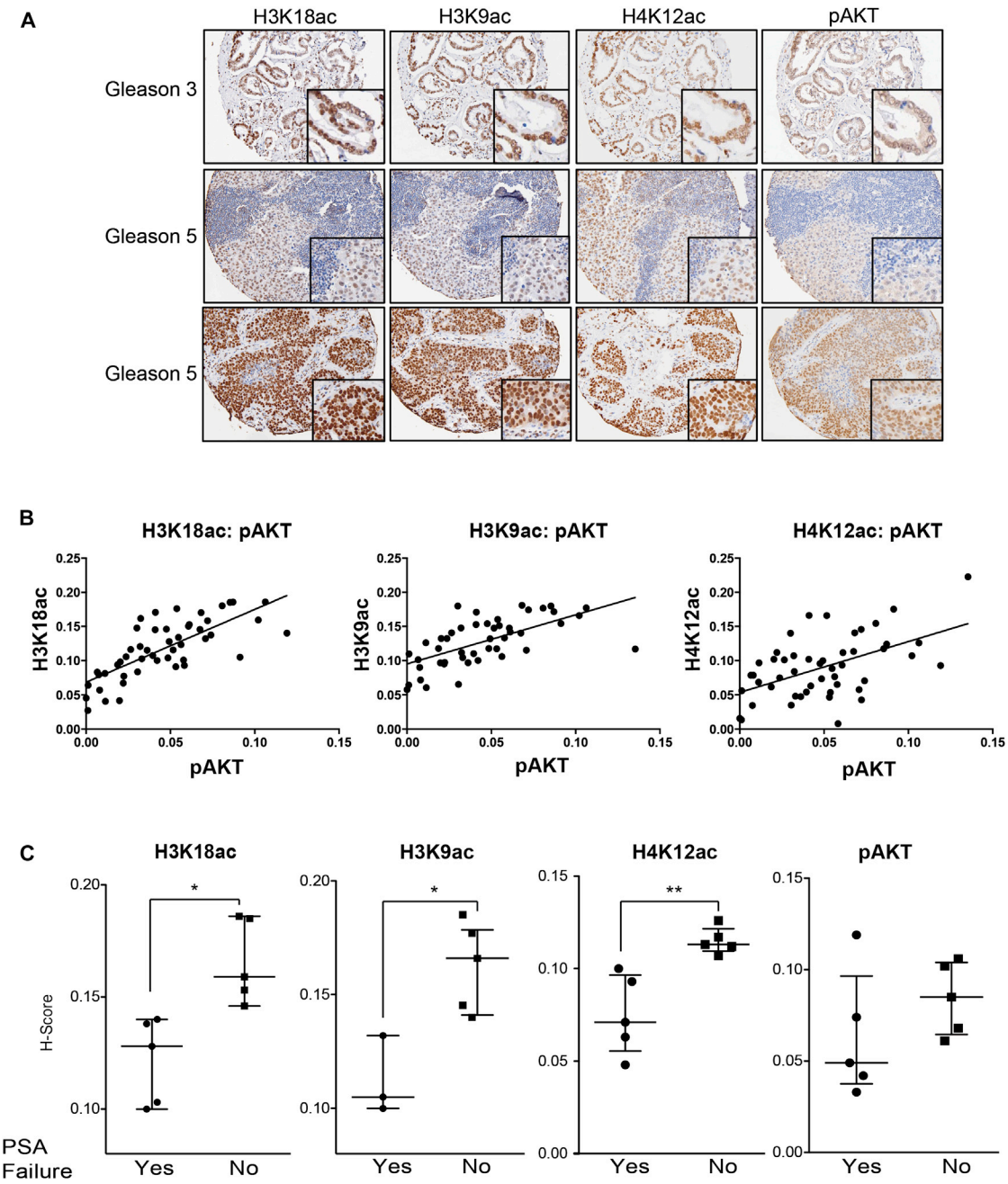

Figure 7. pAKT Correlates with Histone Acetylation Levels in Human Prostate Cancer

(A) Representative images of H3K18ac, H3K9ac, H4K12ac, and pAKT expression detected by immunohistochemistry in Gleason grade 3–5, metastatic (n = 25), and nonmetastatic (n = 24) prostate cancer tumors.

(B) H scores were determined, and correlations between marks were determined. pAKT expression showed a significant correlation with H3K18ac levels ($r = 0.7452$, $p < 0.0001$), H3K9ac ($r = 0.6283$, $p < 0.0001$), and H4K12ac ($r = 0.5276$, $p < 0.0001$).

(C) Box plot showing H scores for H4K12ac, H3K18ac, H3K9ac, and pAKT in prostate cancer tumors in patients that did (Yes) or did not (No) develop PSA failure (**$p < 0.005$, *$p < 0.05$).

of metabolism and epigenetics. The finding that the PI3K/Akt pathway is a key determinant of histone acetylation levels in tumors represents an important step forward in understanding the extent to which oncogenic metabolic reprogramming could control the epigenome.

EXPERIMENTAL PROCEDURES

Reagents and Cell Lines

LN229-myrAkt cells have been previously described (Elstrom et al., 2004). LN229-myrAkt and SF188-myrAkt cells were a gift of C.B. Thompson, MSKCC. LN229-Acly, LN229-S455A, and LN229-S455D and empty vector stable

cell lines were generated by transfecting cells with pEF6, pEF6-Acly(WT), pEF6-Acly(S455A), or pEF6-Acly(S455D) constructs and selecting. See the Supplemental Experimental Procedures for specific culture conditions and information on inhibitors and antibodies used.

YSI Metabolite and Doubling Time Measurements

Glucose and glutamine consumption and lactate production were measured using a YSI 7100 Bioanalyzer. Measurements were conducted over a 24 hr time period and normalized to cell number area under the curve, as previously described (Londoño Gentile et al., 2013). Briefly, metabolite consumption was defined as $v = V(x_{medium\ control} - x_{final})/A$, where v is metabolite consumption/production, V is culture volume, x is metabolite concentration, and A is cell number area under the curve. A was calculated as $N(T)d/ln2(1 - 2^{-T/d})$, where $N(T)$ is the final cell count, d is doubling time, and T is time of experiment. Doubling time was calculated as $d = (T)[log(2)/log(Q2/Q1)]$, where $Q1$ is starting cell number and $Q2$ is final cell number, as determined by manual counting using a hemocytometer.

Mass Spectrometry Analysis of Histones

For ^{12}C study, LN229 cells in triplicate wells were incubated for 24 hr in 1 mM or 10 mM glucose. For ^{13}C study, LN229 cells were first cultured in 1 mM glucose overnight. Triplicate wells of cells were then treated with 1 or 10 mM [U-^{13}C] glucose for 2 or 24 hr. Histones were acid extracted, as described in the Supplemental Experimental Procedures. Total histones were subjected to chemical derivatization using propionic anhydride (Sigma-Aldrich) and digested with sequencing-grade trypsin at a 10:1 substrate:enzyme ratio for 6 hr at 37°C. The digested peptides were treated with an additional round of propionylation for the purpose of adding propionyl group to the newly generated N terminus. Peptides were desalted using C18 extracted mini disk (Empore 3M) and dissolved in 0.1% formic acid. Approximately 1 μg of each sample was loaded via an autosampler (EASY-nLC, Thermo Fisher Scientific) onto a homemade 75 μm reversed-phase analytical column packed with 15 cm C18-AQ resin (3 μm particle sizes, 120 Å pore size) at a rate of 550 nl/min. Peptides were chromatographically resolved on a 66 min 2%–98% solvent B gradient (solvent A = 0.1% formic acid, solvent B = 100% acetonitrile) at a flow rate of 250 nl/min. The eluted peptides were electrosprayed through a PicoTip Emitter (New Objective) and detected by LTQ Orbitrap Velos Mass Spectrometer (Thermo Fisher Scientific). A resolution of 60,000 was used in the Orbitrap for the full mass spectrometry (MS), followed by MS/MS spectra collected in the ion trap.

After the MS data were generated, an in-house program was developed to calculate the relative intensity of ^{13}C-enriched acetyl groups. For example, there are four acetyl groups in histone H4 residues 4–17 (K5/8/12/16), with a 2 Dalton mass shift between adjacent groups. Because the isotope patterns of adjacent groups overlap, the intensity from the former group should be subtracted. After calibration, the intensity of each group divided by the total intensity is the relative intensity.

RNA Sequencing

LN229 cells were incubated for 24 hr in 1 mM or 10 mM glucose, or 1 mM glucose + 5 mM sodium acetate. RNA was isolated using TRIzol reagent and submitted to the Functional Genomics Core at the University of Pennsylvania for library preparation and sequencing. Details of data analysis and clustering may be found in the Supplemental Experimental Procedures.

LC-MS Metabolite Measurements

Acetyl-CoA and CoASH measurements were conducted as previously described (Basu and Blair, 2012; Basu et al., 2011). Detailed protocol is included in the Supplemental Experimental Procedures. For molar concentrations, measurements were normalized to cell volume, as determined using a Coulter Z2 Particle Counter, as previously described (Wellen et al., 2010). Protocol for citrate and glutamate analysis is also described in the Supplemental Experimental Procedures.

Histone Acetylation in Isolated Nuclei Assay

Nuclei were isolated from approximately 9 × 10^6 adherent LN229 cells by using a cell lifter and cold nuclear isolation buffer (NIB) (15 mM Tris-HCL [pH 7.5], 60 mM KCl, 15 mM NaCl, 5 mM $MgCl_2$, 1 mM $CaCl_2$, 250 mM sucrose, 0.1% NP-40). Nuclei were pelleted at 600 RCF (relative centrifugal force) for 5 min in 4°C and followed by two washes using NIB buffer without NP-40. Nuclei were suspended with indicated concentrations of acetyl-CoA and CoASH in 200 μl NIB buffer without NP-40 for 1 hr at 37°C. After incubation, nuclei were pelleted at 600 RCF for 5 min and subjected to acid extraction (described in the Supplemental Experimental Procedures).

Immunohistochemistry and Scoring of Murine Tissues

For histological evaluation, tissue samples were harvested as described (Gunther et al., 2002; Rhim et al., 2012). Immunohistochemistry was performed on paraffin-embedded sections. Tissue sections were dewaxed and rehydrated. Antigen retrieval was performed by boiling samples in citrate buffer (pH 6) for 20 min (for AcH4, AcH3, and H3K4me) or in Tris-EDTA 10 mM buffer (pH 9) for 45 min (pAcly), and endogenous peroxidase was blunted by incubating samples with 3% H_2O_2 for 10 min. After incubation with the primary antibody, slides were rinsed in PBS, and signals were developed using the Vectastain Elite Kit and 3,3′-diaminobenzidine as a substrate for the peroxidase chromogenic reaction (Vector Laboratories). At least three animals/group were evaluated. All animal studies were approved by the University of Pennsylvania Institutional Animal Care and Use Committee (IACUC).

Quantification of AcH4 positivity in acinar cells in Kras WT and KPCY mice (n = 5/group) was performed in a semiautomated manner using ImageJ software. For each animal, 5–10 images from different, nonoverlapping microscopic fields were analyzed. Images containing malignant or premalignant lesions were excluded from the analysis. Count of nuclei within each image was calculated using ImageJ, while positive nuclei were scored by a blinded evaluator. Ductal and islet cells were excluded by the evaluator.

Immunohistochemistry and Automated Scoring for Human Gliomas

Cases were obtained from the University of Pennsylvania following approval from the institutional review board. All cases were deidentified prior to analysis and contained in previously well-characterized tissue microarray sections (Venneti et al., 2013a). The cohort consisted of a total of 56 glioma samples (4 WHO grade II oligodendrogliomas, 5 grade III anaplastic oligodendrogliomas, 6 grade II oligoastrocytomas, 4 grade I pilocytic astrocytomas, 4 grade II diffuse astrocytomas, 9 grade III anaplastic astrocytomas, 14 grade IV glioblastomas, 2 grade I gangliogliomas, and 8 grade II ependymomas). A neuropathologist evaluated all cases. Immunohistochemical studies and quantification were performed as previously described (Venneti et al., 2013b). Details may be found in the Supplemental Experimental Procedures.

Immunohistochemistry and Scoring of Human Prostate Tumors

Cases were obtained from the University of Pennsylvania following institutional review board approval. TMAs were assembled from primary tumors from 49 patients with either metastatic (n = 25) or localized (n = 24) disease. Sections (5 μm) from formalin-fixed paraffin-embedded (FFPE) TMA tissue blocks were prepared for immunohistochemical stain. Details of the staining and scoring are provided in the Supplemental Experimental Procedures.

Statistical Analyses

Student's two-tailed t tests were used for all analyses directly comparing two data sets. For in vitro assay testing AcCoA and CoASH effects on histone acetylation, repeated-measures one-way ANOVA was used, with posttest for linear trend. For correlations shown for human IHC, Pearson's product-moment correlation coefficient (Pearson's r) and corresponding two-tailed significance (p value) were determined.

ACCESSION NUMBERS

Data have been deposited in the GEO database under accession number GSE57488.

SUPPLEMENTAL INFORMATION

Supplemental Information includes Supplemental Experimental Procedures, seven figures, and three tables and can be found with this article online at http://dx.doi.org/10.1016/j.cmet.2014.06.004.

AUTHOR CONTRIBUTIONS

J.V.L. performed and analyzed experiments in glioblastoma cells. A.C. performed and analyzed experiments using mouse tissues and cells from pancreas. S.S. performed and analyzed experiments in prostate cancer cells and assisted in other analyses. E.J. provided technical assistance. N.W.S. and A.J.W. performed LC-MS metabolite analyses, and N.W.S., A.J.W., and I.A.B. analyzed data. S.W. and M.D.F. analyzed human prostate cancer data. S.V. and A.J. generated human glioma TMA, and S.V. analyzed data. S.L. performed histone MS, and Z.-F.Y. and B.A.G. analyzed data. N.M.A. and B.Z.S. provided mouse pancreas sections and assisted in data interpretation. L.A.C. provided mouse mammary tissue sections and assisted in data interpretation. H.-W.L. and K.-J.W. performed RNA-seq data analysis and clustering. N.B.H. and T.R.R. provided prostate cancer patient outcome data. K.E.W. conceived and guided the study, analyzed data, and wrote the manuscript. All authors reviewed data and provided feedback on the manuscript.

ACKNOWLEDGMENTS

This work was supported by grants from the Pew Charitable Trusts (Biomedical Scholar Award), the Elsa U. Pardee Foundation, the American Diabetes Association (7-12-JF-59), and University of Pennsylvania Start-up Funds, to K.E.W. I.A.B. was supported by NIH grants P30ES0138328 and T32ES019851. B.A.G. acknowledges funding from the National Science Foundation Early Faculty CAREER award and an NIH Innovator grant (DP2OD007447) from the Office of the Director. K.-J.W. acknowledges R21-DK098769 and the University of Pennsylvania Diabetes Research Center (DRC) P30-DK19525. We thank George Belka for assistance with mammary tissue sections, as well as Dan Martinez and Li-Ping Wang for technical assistance with human tissue IHC. We thank the Functional Genomics Core at DRC (P30-DK19525) for RNA sequencing.

Received: December 12, 2013
Revised: May 5, 2014
Accepted: May 22, 2014
Published: July 3, 2014

REFERENCES

Albaugh, B.N., Arnold, K.M., and Denu, J.M. (2011). KAT(ching) metabolism by the tail: insight into the links between lysine acetyltransferases and metabolism. ChemBioChem *12*, 290–298.

Azad, N., Zahnow, C.A., Rudin, C.M., and Baylin, S.B. (2013). The future of epigenetic therapy in solid tumours—lessons from the past. Nat Rev Clin Oncol *10*, 256–266.

Basu, S.S., and Blair, I.A. (2012). SILEC: a protocol for generating and using isotopically labeled coenzyme A mass spectrometry standards. Nat. Protoc. *7*, 1–12.

Basu, S.S., Mesaros, C., Gelhaus, S.L., and Blair, I.A. (2011). Stable isotope labeling by essential nutrients in cell culture for preparation of labeled coenzyme A and its thioesters. Anal. Chem. *83*, 1363–1369.

Bauer, D.E., Hatzivassiliou, G., Zhao, F., Andreadis, C., and Thompson, C.B. (2005). ATP citrate lyase is an important component of cell growth and transformation. Oncogene *24*, 6314–6322.

Bianco-Miotto, T., Chiam, K., Buchanan, G., Jindal, S., Day, T.K., Thomas, M., Pickering, M.A., O'Loughlin, M.A., Ryan, N.K., Raymond, W.A., et al.; Australian Prostate Cancer BioResource (2010). Global levels of specific histone modifications and an epigenetic gene signature predict prostate cancer progression and development. Cancer Epidemiol. Biomarkers Prev. *19*, 2611–2622.

Cai, L., Sutter, B.M., Li, B., and Tu, B.P. (2011). Acetyl-CoA induces cell growth and proliferation by promoting the acetylation of histones at growth genes. Mol. Cell *42*, 426–437.

Chervona, Y., and Costa, M. (2012). Histone modifications and cancer: biomarkers of prognosis? Am J Cancer Res *2*, 589–597.

Dawson, M.A., and Kouzarides, T. (2012). Cancer epigenetics: from mechanism to therapy. Cell *150*, 12–27.

Donohoe, D.R., Collins, L.B., Wali, A., Bigler, R., Sun, W., and Bultman, S.J. (2012). The Warburg effect dictates the mechanism of butyrate-mediated histone acetylation and cell proliferation. Mol. Cell *48*, 612–626.

Eisenberg, T., Schroeder, S., Andryushkova, A., Pendl, T., Küttner, V., Bhukel, A., Mariño, G., Pietrocola, F., Harger, A., Zimmermann, A., et al. (2014). Nucleocytosolic depletion of the energy metabolite acetyl-coenzyme a stimulates autophagy and prolongs lifespan. Cell Metab. *19*, 431–444.

Elstrom, R.L., Bauer, D.E., Buzzai, M., Karnauskas, R., Harris, M.H., Plas, D.R., Zhuang, H., Cinalli, R.M., Alavi, A., Rudin, C.M., and Thompson, C.B. (2004). Akt stimulates aerobic glycolysis in cancer cells. Cancer Res. *64*, 3892–3899.

Evertts, A.G., Zee, B.M., Dimaggio, P.A., Gonzales-Cope, M., Coller, H.A., and Garcia, B.A. (2013). Quantitative dynamics of the link between cellular metabolism and histone acetylation. J. Biol. Chem. *288*, 12142–12151.

Fendt, S.M., Bell, E.L., Keibler, M.A., Olenchock, B.A., Mayers, J.R., Wasylenko, T.M., Vokes, N.I., Guarente, L., Vander Heiden, M.G., and Stephanopoulos, G. (2013). Reductive glutamine metabolism is a function of the α-ketoglutarate to citrate ratio in cells. Nat Commun *4*, 2236.

Friis, R.M., Wu, B.P., Reinke, S.N., Hockman, D.J., Sykes, B.D., and Schultz, M.C. (2009). A glycolytic burst drives glucose induction of global histone acetylation by picNuA4 and SAGA. Nucleic Acids Res. *37*, 3969–3980.

Gameiro, P.A., Yang, J., Metelo, A.M., Pérez-Carro, R., Baker, R., Wang, Z., Arreola, A., Rathmell, W.K., Olumi, A., López-Larrubia, P., et al. (2013). In vivo HIF-mediated reductive carboxylation is regulated by citrate levels and sensitizes VHL-deficient cells to glutamine deprivation. Cell Metab. *17*, 372–385.

Guan, K.L., and Xiong, Y. (2011). Regulation of intermediary metabolism by protein acetylation. Trends Biochem. Sci. *36*, 108–116.

Gunther, E.J., Belka, G.K., Wertheim, G.B., Wang, J., Hartman, J.L., Boxer, R.B., and Chodosh, L.A. (2002). A novel doxycycline-inducible system for the transgenic analysis of mammary gland biology. FASEB J. *16*, 283–292.

Hanahan, D., and Weinberg, R.A. (2011). Hallmarks of cancer: the next generation. Cell *144*, 646–674.

Hatzivassiliou, G., Zhao, F., Bauer, D.E., Andreadis, C., Shaw, A.N., Dhanak, D., Hingorani, S.R., Tuveson, D.A., and Thompson, C.B. (2005). ATP citrate lyase inhibition can suppress tumor cell growth. Cancer Cell *8*, 311–321.

Kaelin, W.G., Jr., and McKnight, S.L. (2013). Influence of metabolism on epigenetics and disease. Cell *153*, 56–69.

Katada, S., Imhof, A., and Sassone-Corsi, P. (2012). Connecting threads: epigenetics and metabolism. Cell *148*, 24–28.

Killian, J.K., Kim, S.Y., Miettinen, M., Smith, C., Merino, M., Tsokos, M., Quezado, M., Smith, W.I., Jr., Jahromi, M.S., Xekouki, P., et al. (2013). Succinate dehydrogenase mutation underlies global epigenomic divergence in gastrointestinal stromal tumor. Cancer Discov *3*, 648–657.

Kurdistani, S.K. (2007). Histone modifications as markers of cancer prognosis: a cellular view. Br. J. Cancer *97*, 1–5.

Langer, M.R., Fry, C.J., Peterson, C.L., and Denu, J.M. (2002). Modulating acetyl-CoA binding in the GCN5 family of histone acetyltransferases. J. Biol. Chem. *277*, 27337–27344.

Letouzé, E., Martinelli, C., Loriot, C., Burnichon, N., Abermil, N., Ottolenghi, C., Janin, M., Menara, M., Nguyen, A.T., Benit, P., et al. (2013). SDH mutations establish a hypermethylator phenotype in paraganglioma. Cancer Cell *23*, 739–752.

Lino, M.M., and Merlo, A. (2011). PI3Kinase signaling in glioblastoma. J. Neurooncol. *103*, 417–427.

Londoño Gentile, T., Lu, C., Lodato, P.M., Tse, S., Olejniczak, S.H., Witze, E.S., Thompson, C.B., and Wellen, K.E. (2013). DNMT1 is regulated by ATP-citrate lyase and maintains methylation patterns during adipocyte differentiation. Mol. Cell. Biol. *33*, 3864–3878.

Losman, J.A., and Kaelin, W.G., Jr. (2013). What a difference a hydroxyl makes: mutant IDH, (R)-2-hydroxyglutarate, and cancer. Genes Dev. *27*, 836–852.

Lu, C., and Thompson, C.B. (2012). Metabolic regulation of epigenetics. Cell Metab. *16*, 9–17.

Lu, C., Ward, P.S., Kapoor, G.S., Rohle, D., Turcan, S., Abdel-Wahab, O., Edwards, C.R., Khanin, R., Figueroa, M.E., Melnick, A., et al. (2012). IDH mutation impairs histone demethylation and results in a block to cell differentiation. Nature *483*, 474–478.

Lum, J.J., Bauer, D.E., Kong, M., Harris, M.H., Li, C., Lindsten, T., and Thompson, C.B. (2005). Growth factor regulation of autophagy and cell survival in the absence of apoptosis. Cell *120*, 237–248.

Luo, W., and Semenza, G.L. (2012). Emerging roles of PKM2 in cell metabolism and cancer progression. Trends Endocrinol. Metab. *23*, 560–566.

Mariño, G., Pietrocola, F., Eisenberg, T., Kong, Y., Malik, S.A., Andryushkova, A., Schroeder, S., Pendl, T., Harger, A., Niso-Santano, M., et al. (2014). Regulation of autophagy by cytosolic acetyl-coenzyme A. Mol. Cell *53*, 710–725.

Martinez-Pastor, B., Cosentino, C., and Mostoslavsky, R. (2013). A tale of metabolites: the cross-talk between chromatin and energy metabolism. Cancer Discov *3*, 497–501.

McBrian, M.A., Behbahan, I.S., Ferrari, R., Su, T., Huang, T.W., Li, K., Hong, C.S., Christofk, H.R., Vogelauer, M., Seligson, D.B., and Kurdistani, S.K. (2013). Histone acetylation regulates intracellular pH. Mol. Cell *49*, 310–321.

Migita, T., Narita, T., Nomura, K., Miyagi, E., Inazuka, F., Matsuura, M., Ushijima, M., Mashima, T., Seimiya, H., Satoh, Y., et al. (2008). ATP citrate lyase: activation and therapeutic implications in non-small cell lung cancer. Cancer Res. *68*, 8547–8554.

Morris, J.P., 4th, Wang, S.C., and Hebrok, M. (2010). KRAS, Hedgehog, Wnt and the twisted developmental biology of pancreatic ductal adenocarcinoma. Nat. Rev. Cancer *10*, 683–695.

Potapova, I.A., El-Maghrabi, M.R., Doronin, S.V., and Benjamin, W.B. (2000). Phosphorylation of recombinant human ATP:citrate lyase by cAMP-dependent protein kinase abolishes homotropic allosteric regulation of the enzyme by citrate and increases the enzyme activity. Allosteric activation of ATP:citrate lyase by phosphorylated sugars. Biochemistry *39*, 1169–1179.

Rhim, A.D., Mirek, E.T., Aiello, N.M., Maitra, A., Bailey, J.M., McAllister, F., Reichert, M., Beatty, G.L., Rustgi, A.K., Vonderheide, R.H., et al. (2012). EMT and dissemination precede pancreatic tumor formation. Cell *148*, 349–361.

Seligson, D.B., Horvath, S., Shi, T., Yu, H., Tze, S., Grunstein, M., and Kurdistani, S.K. (2005). Global histone modification patterns predict risk of prostate cancer recurrence. Nature *435*, 1262–1266.

Shen, H., and Laird, P.W. (2013). Interplay between the cancer genome and epigenome. Cell *153*, 38–55.

Shi, L., and Tu, B.P. (2013). Acetyl-CoA induces transcription of the key G1 cyclin CLN3 to promote entry into the cell division cycle in Saccharomyces cerevisiae. Proc. Natl. Acad. Sci. USA *110*, 7318–7323.

Son, J., Lyssiotis, C.A., Ying, H., Wang, X., Hua, S., Ligorio, M., Perera, R.M., Ferrone, C.R., Mullarky, E., Shyh-Chang, N., et al. (2013). Glutamine supports pancreatic cancer growth through a KRAS-regulated metabolic pathway. Nature *496*, 101–105.

Takahashi, H., McCaffery, J.M., Irizarry, R.A., and Boeke, J.D. (2006). Nucleocytosolic acetyl-coenzyme a synthetase is required for histone acetylation and global transcription. Mol. Cell *23*, 207–217.

Ulanovskaya, O.A., Zuhl, A.M., and Cravatt, B.F. (2013). NNMT promotes epigenetic remodeling in cancer by creating a metabolic methylation sink. Nat. Chem. Biol. *9*, 300–306.

Vander Heiden, M.G. (2011). Targeting cancer metabolism: a therapeutic window opens. Nat. Rev. Drug Discov. *10*, 671–684.

Venneti, S., Felicella, M.M., Coyne, T., Phillips, J.J., Gorovets, D., Huse, J.T., Kofler, J., Lu, C., Tihan, T., Sullivan, L.M., et al. (2013a). Histone 3 lysine 9 trimethylation is differentially associated with isocitrate dehydrogenase mutations in oligodendrogliomas and high-grade astrocytomas. J. Neuropathol. Exp. Neurol. *72*, 298–306.

Venneti, S., Garimella, M.T., Sullivan, L.M., Martinez, D., Huse, J.T., Heguy, A., Santi, M., Thompson, C.B., and Judkins, A.R. (2013b). Evaluation of histone 3 lysine 27 trimethylation (H3K27me3) and enhancer of Zest 2 (EZH2) in pediatric glial and glioneuronal tumors shows decreased H3K27me3 in H3F3A K27M mutant glioblastomas. Brain Pathol. *23*, 558–564.

Ward, P.S., and Thompson, C.B. (2012). Metabolic reprogramming: a cancer hallmark even warburg did not anticipate. Cancer Cell *21*, 297–308.

Wellen, K.E., Hatzivassiliou, G., Sachdeva, U.M., Bui, T.V., Cross, J.R., and Thompson, C.B. (2009). ATP-citrate lyase links cellular metabolism to histone acetylation. Science *324*, 1076–1080.

Wellen, K.E., Lu, C., Mancuso, A., Lemons, J.M., Ryczko, M., Dennis, J.W., Rabinowitz, J.D., Coller, H.A., and Thompson, C.B. (2010). The hexosamine biosynthetic pathway couples growth factor-induced glutamine uptake to glucose metabolism. Genes Dev. *24*, 2784–2799.

Xiao, M., Yang, H., Xu, W., Ma, S., Lin, H., Zhu, H., Liu, L., Liu, Y., Yang, C., Xu, Y., et al. (2012). Inhibition of α-KG-dependent histone and DNA demethylases by fumarate and succinate that are accumulated in mutations of FH and SDH tumor suppressors. Genes Dev. *26*, 1326–1338.

Ying, H., Kimmelman, A.C., Lyssiotis, C.A., Hua, S., Chu, G.C., Fletcher-Sananikone, E., Locasale, J.W., Son, J., Zhang, H., Coloff, J.L., et al. (2012). Oncogenic Kras maintains pancreatic tumors through regulation of anabolic glucose metabolism. Cell *149*, 656–670.

Yun, J., Johnson, J.L., Hanigan, C.L., and Locasale, J.W. (2012). Interactions between epigenetics and metabolism in cancers. Front Oncol *2*, 163.